J Musculoskelet Neuronal Interact 2014; 14(4):473-483

Original Article

Hylonome

Growth hormone mitigates loss of periosteal bone formation and muscle mass in disuse osteopenic rats

M-C. Grubbe[1,2], J.S. Thomsen[1], J.R. Nyengaard[3], M. Duruox[2], A. Brüel[1]

[1]Department of Biomedicine, Aarhus University, Aarhus, Denmark; [2]Laboratory for Cancer biology, Biomedicine, Aalborg University, Aalborg, Denmark; [3]Stereology and EM Laboratory, Centre for Stochastic Geometry and Advanced Bioimaging Aarhus University Hospital, Aarhus, Denmark

Abstract

Growth hormone (GH) is a potent anabolic agent capable of increasing both bone and muscle mass. The aim was to investigate whether GH could counteract disuse-induced loss of bone and muscle mass in a rat model. Paralysis was induced by injecting 4 IU Botox (BTX) into the muscles of the right hind limb. Sixty female Wistar rats, 14 weeks old, were divided into the following groups: baseline, controls, BTX, BTX+GH, and GH. GH was given at a dosage of 5 mg/kg/d for 4 weeks. Compared with controls, BTX resulted in lower periosteal bone formation rate (BFR/BS, –79%, $P<0.001$), bone mineral density (aBMD, –13%, $P<0.001$), trabecular bone volume (BV/TV, –26%, $P<0.05$), and mid-femoral bone strength (–12%, $P<0.05$). In addition, BTX reduced rectus femoris muscle mass (–69%, $P<0.001$) and muscle cell cross sectional area (CSA) (–73%, $P<0.001$) compared with controls. GH counteracted disuse-induced losses of periosteal BFR/BS (2-fold increase vs. BTX, $P<0.001$), whereas no effect on aBMD, trabecular BV/TV, or bone strength was found. In addition, GH partly prevented loss of muscle mass (+29% vs. BTX, $P<0.001$), and tended to prevent loss of muscle CSA (+11%, $P=0.064$). In conclusion, GH mitigates disuse-induced loss of periosteal BFR/BS at the mid-femur and rectus femoris muscle mass.

Keywords: Growth Hormone, Disuse, Rat, Mechanics, Histomorphometry

Introduction

Musculoskeletal diseases are one of the most common causes of chronic disabilities, and loss of bone and muscle is a growing issue in relation to public health[1-3]. Mechanical loading is an important factor controlling bone and muscle mass[4,5]. Unloading leads to significant loss of bone and muscle mass, which may result in osteoporosis and sarcopenia in bedridden patients, patients with spinal cord injuries, and astronauts[6-8]. Thus, prolonged bed rest studies in humans have shown reduced BMD of the lumbar spine, hip, and lower extremities, and decreased trabecular BV/TV and trabecular thickness[7,9].

In 2001, Chappard et al. described a model, where botulinum toxin A (BTX) was used to paralyze the hind limb musculature in rats in order to study the effect of disuse on the skeleton[10]. In the motor endplates, BTX inhibits the release of acetylcholine from the pre-synaptic motor nerve terminals. Subsequently, action potentials from the motor nerve can no longer be transmitted to the muscle, and paralysis of the muscle is thereby induced. In rodents, we found that this paralysis leads to substantially reduced muscle mass of the affected limb followed by decreased bone mass and loss of bone strength[11,12]. Furthermore, this condition results in a significant decrease of mineralising surfaces and bone formation at the periosteal bone surface[11,12].

Growth hormone (GH) is an important regulator of postnatal growth and bone mass, and exerts its effect either directly or indirectly via IGF-I. GH stimulates the liver to produce and secrete IGF-I, and, in addition, many peripheral tissues also produce IGF-I including bone and skeletal muscles[13,14]. Locally produced IGF-I acts in an autocrine/paracrine manner. *In vitro* studies of osteoblasts show that GH can increase DNA synthesis, cell proliferation, and production of alkaline phosphatase and type I collagen[15,16]. Likewise, it has been found that IGF-I increases osteoblast activity and proliferation[17,18].

The authors have no conflict of interest.

Corresponding author: Annemarie Brüel, Department of Biomedicine, Wilhelm Meyers Allé 3, Building 1233, Aarhus University, DK-8000 Aarhus C, Denmark
E-mail: mb@ana.au.dk

Edited by: S. Warden
Accepted 5 October 2014

Experimental studies shows that GH can increase bone mass and enhance mechanical strength of bone in both intact and osteopenic rodents[19-21], mainly due to a pronounced increase in the formation of new bone at the periosteal surfaces[19,21]. Furthermore, GH is a potent anabolic agent known to promote skeletal muscle cell protein synthesis and growth[22]. Several studies in rodents have shown that GH can induce a substantial increase in muscle mass[23,24]. Thus, GH is a proven anabolic factor capable of increasing both bone and muscle mass.

In GH-treated hypophysectomised rats, skeletal unloading completely prevents increase in trabecular bone volume, and severely inhibits periosteal bone formation[25], and the response to GH in terms of increase in local production/content of IGF-I seems to be site dependent[26]. Furthermore, in GH-deficient dwarf rats it has been shown that skeletal unloading inhibits activation of IGF-I signalling pathways, which thereby leads to IGF-I resistance[27]. However, it should be noted that hypophysectomy leads to absence of other pituitary hormones including thyroxin and sex hormones, as well as a substantial weight loss.

Therefore, the aim of the present experiment was to investigate whether GH could counteract paralysis-induced bone loss in normal rats assessed by bone strength, bone micro-architecture, and bone turnover. Furthermore, the purpose was to study whether paralysis-induced loss of muscle mass could be attenuated by GH administration.

Materials and methods

Animal, design, and drug administration

Sixty female Wistar rats, 14 weeks old, were randomized by weight into 5 experimental groups with 12 animals in each group: baseline, control, BTX, BTX+GH, and GH. The rats were anaesthetized with 3% isoflurane (Isoflurane, Baxter, Deerfield, IL), and the right hind limb was shaved. Botulinum toxin type A (Botox, Allergan, County Mayo, Ireland) was dissolved in saline at a concentration of 20 units/ml. The right hind limb of each animal was injected (im) with a total of 4 units of BTX distributed as 1 unit into the following locations: the upper part of quadriceps, the lower part of quadriceps, the hamstrings, and the calf muscles. The rats were monitored during recovery from the anaesthesia, and the following hours in order to detect unwanted side effects.

Human growth hormone (Norditropin, Novo Nordisk, Gentofte, Denmark) was given as subcutaneous (sc) injections 5 times weekly two times a day, at a dosage of 5 mg/kg/d starting at the day of the BTX-injections. The control group and the BTX group were injected with saline. The GH dosing regimen was based upon the findings of Ortoft et al.[19,20]. The animals were injected intraperitoneally (ip) with alizarin red (20 mg/kg, Sigma-Aldrich, St. Louis, MO) 6 day prior to study start, and tetracycline (20 mg/kg, Sigma-Aldrich, St. Louis, MO) and calcein (15 mg/kg, Sigma-Aldrich, St. Louis, MO) 10 and 3 days before termination of the study, respectively.

The gait ability of 6 animals in each group was assessed in the morning at day –1, 1, 2, and thereafter twice a week using a gait ability score originally designed for mice[28]. The animals were group-housed with a cycle of 12 h of light and 12 h of darkness. Standard rat chow (Altromin 1324, Brogaarden, Lynge, Denmark) and tap water were provided *ad libitum* at a freely accessible level in the cages. The animals were weighed at the beginning of the experiment and thereafter once a week.

The experiment lasted for 4 weeks, after which the animals were anaesthetized with 3% isoflurane as inhalation and killed with an overdose of 200 mg/kg pentobarbital (ip) (Mebumal, SAD, Copenhagen, Denmark). Blood was obtained from vena cava inferior, serum isolated, and stored at –80°C. The left and right rectus femoris as well as the right sternocleidomastoid muscle were isolated and the wet weight (WW) determined. The rectus femoris muscles were immersion-fixed in 0.1 M sodium phosphate buffered formaldehyde (4% formaldehyde, pH 7.0) for 48 h. The femora were carefully cleaned from all soft connective tissue, and stored in Ringer's solution at –20°C for the subsequent analyses.

The experiment complied with the EU Directive 2010/63/EU for animal experiments, and was approved by the Danish Animal Experiments Inspectorate.

Determination of total IGF-I in serum

The total IGF-I levels were assayed using a commercially available ELISA kit (Quantikine # MG100, R&D Systems, Minneapolis, MN). The ELISA was performed according to the manufacturer's instructions, and standards, controls, and samples were tested in duplicate. The microplate was read at a wavelength of 460 nm with wavelength correction at 560 nm in a Victor 1420 multilabel spectrophotometer (Wallac, Turku, Finland). The total IGF-I serum concentrations were determined from the standard curve by matching the absorbance readings with the corresponding IGF-1 concentrations. The sensitivity of the kit was 8.4 pg/ml, intra-assay precision was 5.6%, and the inter-assay precision was 9%.

Average muscle cell cross sectional area (CSA)

The central part of the rectus femoris muscle was embedded in methylmethacrylate (Technovit 7100, Kulzer, Germany). Two-µm-thick sections were cut using a microtome (Jung RM2065, Leica Instruments, Germany) and stained with Masson Trichrome. The mean muscle cell cross sectional area (CSA) was determined using a microscope (Nikon Eclipse 80i, Japan) with a motorized specimen stage (Prior 138, Cambridge, England) and a digital camera (Olympus DP72, Tokyo, Japan) connected to a computer with NewCAST software (Visiopharm, Hørsholm, Denmark). Each section was sampled using systematic uniformly random sampling[29]. That is, from a random starting point a new field of view was sampled with a fixed *x*- and *y*-distance from the previous field of view by use of the motorized stage. Using a 2D unbiased counting frame, the striated muscle cell profiles within the counting frame and not touching the exclusion lines were sampled. On average 200 muscle cell profiles were sampled for each animal. At a total magnification of ×1180 the CSA of the individ-

ual muscle cell profiles was estimated using the 2D nucleator principle[30]. In brief, the centre of each muscle cell profile was marked, 4 intercept lines radiating from the centre point was automatically drawn, and the intersections between the cell membrane and the intercept lines were marked interactively. From this the CSA of each muscle cell profile was automatically estimated. The investigator was blinded for the group distribution during the evaluation.

Dual Energy X-ray Absorptiometry (DEXA)

The femora were placed in a pDEXA scanner (Sabre XL, Norland Stratec, Pforzheim, Germany) and scanned using a pixel size of 0.5 mm × 0.5 mm. Bone mineral content (BMC) and areal bone mineral density (aBMD) were determined. Quality assurance was performed by scans of the two solid state phantoms provided with the scanner. The coefficient of variation (CV) of rat femur aBMD is 2.8% in our laboratory.

Mechanical testing

The length of the femora was measured with an electronic caliper, and the midpoint was marked. The maximum load of the mid-femur (three-point-bending test), the femoral head (compression test), and the distal femoral metaphysis (compression test) was determined as previously described in detail[11]. After the three point bending test, an approximately 4-mm-high specimen with plano-parallel ends was sawn from the distal part of the femoral metaphysis just above the uppermost part of the patellofemoral joint cartilage with a diamond precision saw (Exakt Apparatebau, Norderstedt, Germany).

Micro Computed Tomography (μCT)

Before the mechanical testing, the distal femoral metaphysis were scanned using a desktop μCT scanner (Scanco μCT 35, Scanco Medical AG, Brüttisellen, Switzerland) in high resolution mode (1000 projections/180°) with a spatial resolution of 6 × 6 × 6 μm^3, an X-ray tube voltage of 70 kVp and current of 114 μA, and an integration time of 800 ms. A 3.3-mm-high volume of interest, including trabecular bone, but excluding cortical bone and primary spongiosa, was semi manually drawn on each specimen excluding a region of 100 μm adjacent to the top and bottom of the specimens in order to exclude sawing residues. The 3D data sets were low-pass filtered using a Gaussian filter (σ= 1.3, support= 2) and segmented with a fixed threshold filter (642.6 mg HA/cm^3) according to current guidelines[31]. The minimum point between the marrow and the bone peak in the attenuation histogram was automatically determined using IPL (version 5.11, Scanco Medical AG, Brüttisellen, Switzerland) for 5 femora from each group, and the median of these thresholds was used for all segmentations. The structural evaluation was carried out using the software provided with the μCT scanner (version 6.0, Scanco Medical AG, Brüttisellen, Switzerland).

The micro-structural measures included: BV/TV, Tb.Th, Tb.Sp, Tb.N, CD, SMI, and vBMD. The computation of these structural measures has previously been described in detail[32].

Static bone histomorphometry

Mid-diaphyseal sections with a mean thickness of 134 μm were sawed off the proximal part of the femoral diaphysis as close as possible to the fracture point from the three-point bending, and bone area, marrow area, tissue area were determined as previously described[11].

Dynamic bone histomorphometry

For cortical dynamic histomorphometry the mid-diaphyseal cross sections used for static bone histomorphometry were mounted on glass slides. Using the above mentioned microscope, digital images were projected onto a computer monitor with a star-shaped grid with 16 radiating arms superimposed. The grid was placed in the centre of the medullar cavity, so that the radiating lines of the grid randomly intersected the endosteal and periosteal perimeter[33]. At a magnification of ×1180 the number of intersections with either single labels (calcein or tetracycline) or double labels at either the endosteal or periosteal surface was counted. In case of intersection with a double label the distance between the labels was determined using the ruler function in NewCAST. In accordance with current guidelines, the mineral appositional rate (MAR) was calculated as the distance between the labels divided by the interlabeling period, the mineralizing surfaces (MS/BS) were calculated as the number of intersections with doubles labels plus half the number of intersections with single labels divided by the total number of intersections with bone surfaces, and the bone formation rate (BFR/BS) was determined as MAR × MS/BS[34]. Furthermore, in order to estimate whether resorption of bone present at study start took place during the experimental period, the number of intersections with alizarin labels (Ali.S/BS) was also counted[35].

Statistics

Data are presented as mean ± SD. Differences between all groups except GH were evaluated using One Way ANOVA followed by Holm-Sidak test for multiple comparisons. In case of variance in homogeneity or that data were not normally distributed (Shapiro-Wilk test), ANOVA on ranks followed by Dunn's test was applied (this was the case for: 3-point bending test, Tp.Sp, CD, periosteal MS/BS, endosteal MS/BS, MAR, and BFR/BS). GH was compared with controls using a Student's t-test. Differences were considered significant at $P<0.05$.

Results

Body weight, femur length, muscle weight and serum IGF-I

The body weight of the BTX-injected animals decreased with 9% during the first 2 weeks of the experiment, and thereafter increased slightly (Figure 1A and Table 1). For all time points except at the start of the experiment, the body weight of the BTX groups was significantly lower than that of the controls. In contrast, BTX+GH maintained BW at a level not significantly different from the controls. GH alone induced a

	Baseline	Control	BTX	BTX+GH	GH
No. of rats	12	12	12	12	12
Initial BW	230	230	234	232	234
(g)	(8)	(10)	(8)	(9)	(9)
Final BW		249	221***	256$^{\#\#\#}$	302***
(g)	-	(8)	(4)	(13)	(16)
Femur length	33.0***	34.0	33.7†	35.4***,$^{\#\#\#,\dagger\dagger\dagger}$	35.4***,$^{\#\#\#}$
(mm)	(0.71)	(0.51)	(0.59)	(0.69)	(0.58)
Serum IGF-I		562	558	1223**,$^{\#\#}$	1240**
(µg/l)	-	(282)	(174)	(758)	(554)
M. sternocleido-mastoideus (mg)	242	247	220 **,†	257$^{\#\#\#}$	294***
	(17)	(21)	(15)	(28)	(18)

***: P<0.01 vs. control, ***: P<0.001 vs. control, $^{\#\#}$: P<0.01 vs. BTX, $^{\#\#\#}$: P<0.001 vs. BTX, †: P<0.05 vs. baseline, †††: P<0.001 vs. base*line.

Table 1. Number of rats, initial and final body weight (BW), femur length, serum IGF-I, and m. sternocleidomastoideus in rats with BTX induced right hind limb paralysis treated with GH (5 mg/kg/d). Mean (SD).

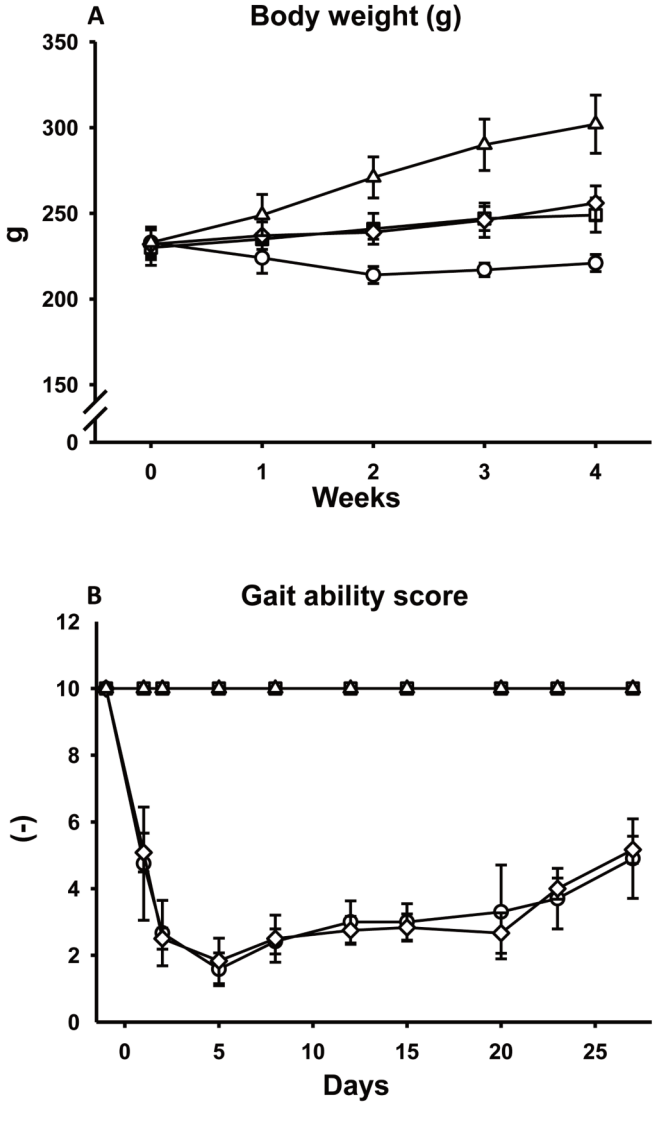

Figure 1. Body weight and gait ability score of rats with BTX induced hind limb paralysis treated with GH (5 mg/kg/d). Mean±SD. □: control, ○: BTX, ◇: BTX+GH, △: GH.

substantial increase in body weight during the experiment, and the final body weight was 29% higher than in controls (P<0.001).

The gait ability score was 10 (maximum) in all animals prior to BTX injection (Figure 1B). However, already at day 1 after the BTX injections the gait ability of the BTX group was severely affected, reaching a minimum score of 1.6±0.49 at day 5. Hereafter, the gait ability score increased gradually to 4.9±1.19 at the end of the study. There was no difference in gait ability score between BTX and BTX+GH at any time point. Controls and GH scored maximum point at all time points.

BTX did not influence longitudinal growth, as no differences in femur length were found, when comparing BTX to controls (Table 1). However, the femur length was significantly higher in the GH and BTX+GH groups compared with controls.

GH treatment resulted in a 2-fold higher level of serum IGF-I in the GH group (1223±758 µg/l, P<0.01) and the BTX+GH group (1240±554 µg/l, P<0.05) after 4 weeks of treatment compared with the control group (562±282 µg/l). BTX alone (558±174 µg/l) did not influence serum IGF-I compared with controls.

Muscle weights and muscle cell CSA

The WW of the right m. rectus femoris was lower in BTX (–69%, P<0.001) and BTX+GH (–59%, P<0.001), when compared with controls (Figure 2A). However, the WW of the right m. rectus femoris was 29% higher in BTX+GH (P<0.001) compared with BTX. GH alone induced a 19% increase in WW of the right m. rectus femoris compared with controls (P<0.001). Mean muscle cell CSA was 73% lower in BTX and 69% lower in BTX+GH compared with controls (P<0.001) (Figure 3B and Table 1). Muscle cell CSA was 11% higher in BTX+GH compared with BTX, however this finding was not significant (P=0.064). In GH alone the muscle cell CSA was 12% higher than controls (P<0.01).

The WW of the sternocleidomastoid muscle was lower in BTX when compared with controls (–11%, P<0.01) and base-

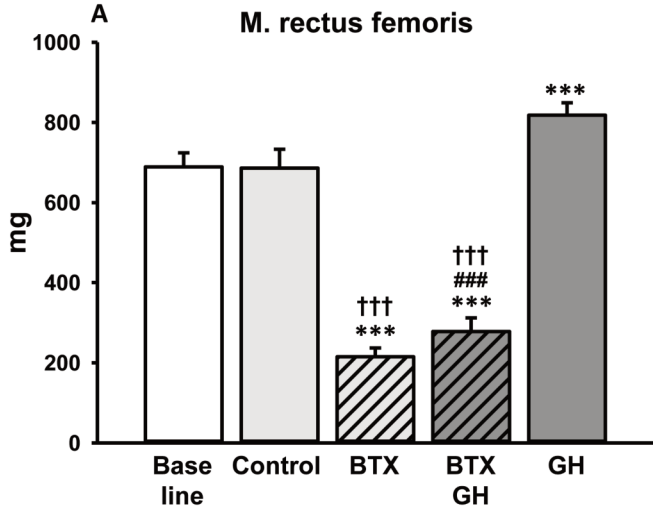

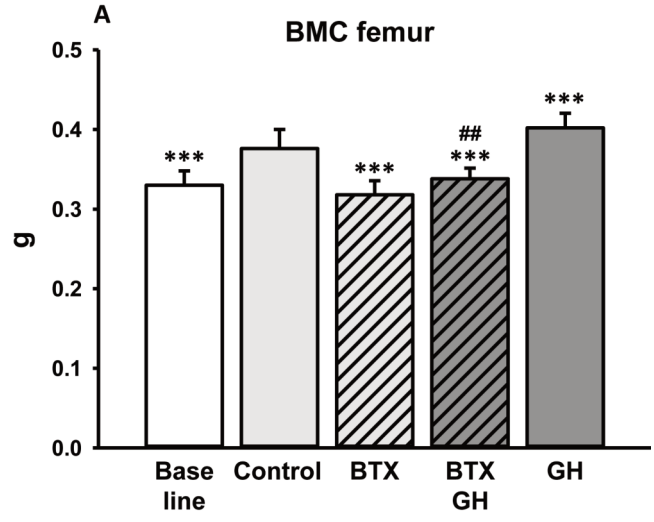

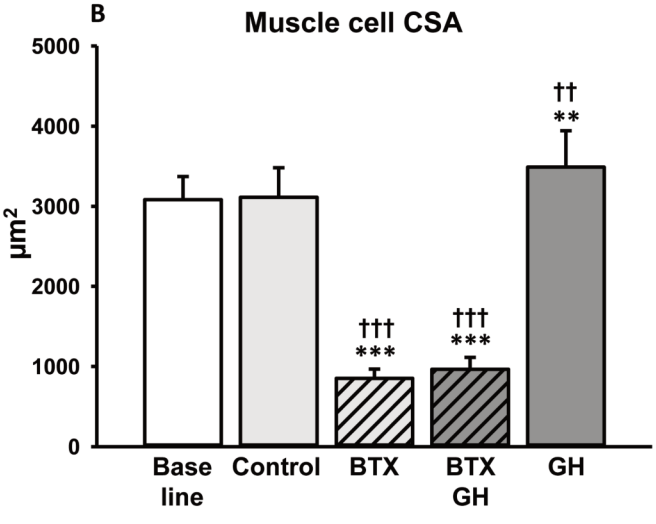

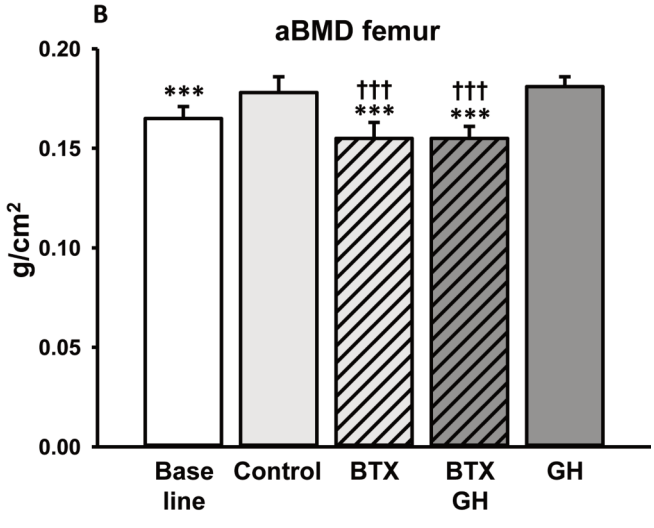

Figure 2. Muscle mass (A) and muscle cell CSA (B) of the rectus femoris muscle in rats with BTX induced hind limb paralysis treated with GH (5 mg/kg/d). Mean ± SD. **: $P<0.01$ vs. control, ***: $P<0.001$ vs. control, ###: $P<0.001$ vs. BTX, ††: $P<0.01$ vs. baseline, †††: $P<0.001$ vs. baseline.

Figure 3. BMC (A) and aBMD (B) of the right femur in rats with BTX induced hind limb paralysis treated with GH (5 mg/kg/d). Mean±SD. ***: $P<0.001$ vs. control, ##: $P<0.01$ vs. BTX, †††: $P<0.001$ vs. baseline.

line (–9%, $P<0.05$), and was 19% higher ($P<0.001$) in GH compared with controls (Table 1).

DEXA

BMC of the right femur was lower in BTX (–15%, $P<0.001$) and BTX+GH (–10%, $P<0.001$) compared with controls, whereas no difference were found when compared to baseline (Figure 3A). BMC was higher in BTX+GH (+6%, $P<0.01$) than in BTX. In GH alone BMC was 7% higher compared with controls ($P<0.001$).

aBMD was not only significant lower (–13%, $P<0.001$) in BTX than in controls, but also significantly lower than in baseline (–6%, $P<0.001$) (Figure 3B). GH did not influence aBMD in neither BTX-injected nor in non-paralysed animals.

Biomechanics

BTX resulted in a lower maximum load of the mid-femoral diaphysis (–12%, $P<0.05$), femoral neck (–17%, $P<0.05$), and distal femoral metaphysis (–25%, $P<0.001$) compared with controls (Table 2). No differences were found between BTX and BTX+GH. Furthermore, the maximum load of the femoral neck and the distal femoral metaphysis were lower in BTX and BTX+GH than in the baseline group. GH alone did not influence maximum load at any of the tested bone sites.

µCT of trabecular bone

At the distal femoral metaphysis trabecular BV/TV (–26%, $P<0.05$), Tb.Th (–16%, $P<0.001$), and vBMD (–22%, $P<0.05$)

F_{max} (N)	Baseline	Control	BTX	BTX+GH	GH
Mid-femur	109	119	105*	112	116
	(7)	(9)	(12)	(15)	(10)
Femoral neck	90	88	73*,†	67**,††	88
	(18)	(8)	(15)	(12)	(10)
Distal femoral metaphysis	719*	828	620***,†	605***,†	865
	(76)	(107)	(113)	(101)	(105)

**: P<0.05 vs. control, **: P<0.01 vs. control, ***: P<0.001 vs. control, †: P<0.05 vs. baseline ††: P<0.01 vs. baseline.*

Table 2. Maximum strength (F_{max}) of the mid-femur, the femoral neck and the distal femoral metaphysis in rats with BTX induced right hind limb paralysis treated with GH (5 mg/kg/d). Mean (SD).

	Baseline	Control	BTX	BTX+GH	GH
BV/TV	0.157	0.189	0.139 *	0.158	0.186
(-)	(0.037)	(0.041)	(0.044)	(0.033)	(0.043)
Tb.Th*	62.9	67.6	56.6 ***,†††	55.9 ***,†††	65.9
(μm)	(4.7)	(4.6)	(4.6)	(6.7)	(4.6)
Tb.N*	3.38	3.49	3.33	3.86	3.55
(mm^{-1})	(0.65)	(0.68)	(0.78)	(0.62)	(0.63)
Tb.Sp*	295	292	306	244	277
(μm)	(7)	(8)	(11)	(3)	(6)
CD	103	101	99	135	116
(mm^3)	(30)	(27)	(37)	(45)	(29)
BMD	246	293	229*	258	289
(mg/cm^3)	(49)	(49)	(59)	(42)	(53)

**: P<0.05 vs. control, ***: P<0.001 vs. control, †††: P<0.001 vs. baseline.*

Table 3. μCT data on trabecular bone from the distal femoral metaphysis in rats with BTX induced right hind limb paralysis treated with GH (5 mg/kg/d). Mean (SD).

	Baseline	Control	BTX	BTX+GH	GH
Tissue area	7.68	8.06	7.72	7.90	8.18
(mm^2)	(0.47)	(0.50)	(0.36)	(0.45)	(0.55)
Bone area	5.24	5.53	5.09*	5.25	5.79
(mm^2)	(0.30)	(0.31)	(0.31)	(0.29)	(0.43)
Marrow area	2.44	2.53	2.64	2.64	2.39
(mm^2)	(0.30)	(0.39)	(0.29)	(0.37)	(0.45)

**: P<0.05 vs. control.*

Table 4. Static histomorphometry on cortical bone from the mid-femur in rats with BTX induced right hind limb paralysis treated with GH (5 mg/kg/d). Mean (SD).

were lower in BTX compared to controls (Table 3). Tb.Th was 17% lower (P<0.001) in BTX+GH when compared with controls, whereas no differences in BV/TV and vBMD was found between these two groups. Furthermore, no differences between any of the groups were found in Tb.N, Tb.Sp, and CD.

Static bone histomorphometry of cortical bone

At the femoral mid-diaphysis the cross sectional bone area was significantly lower in BTX (–8%, P<0.01) compared to controls (Table 4). The cross sectional bone area of BTX+GH did not differ from either BTX or the controls. Furthermore,

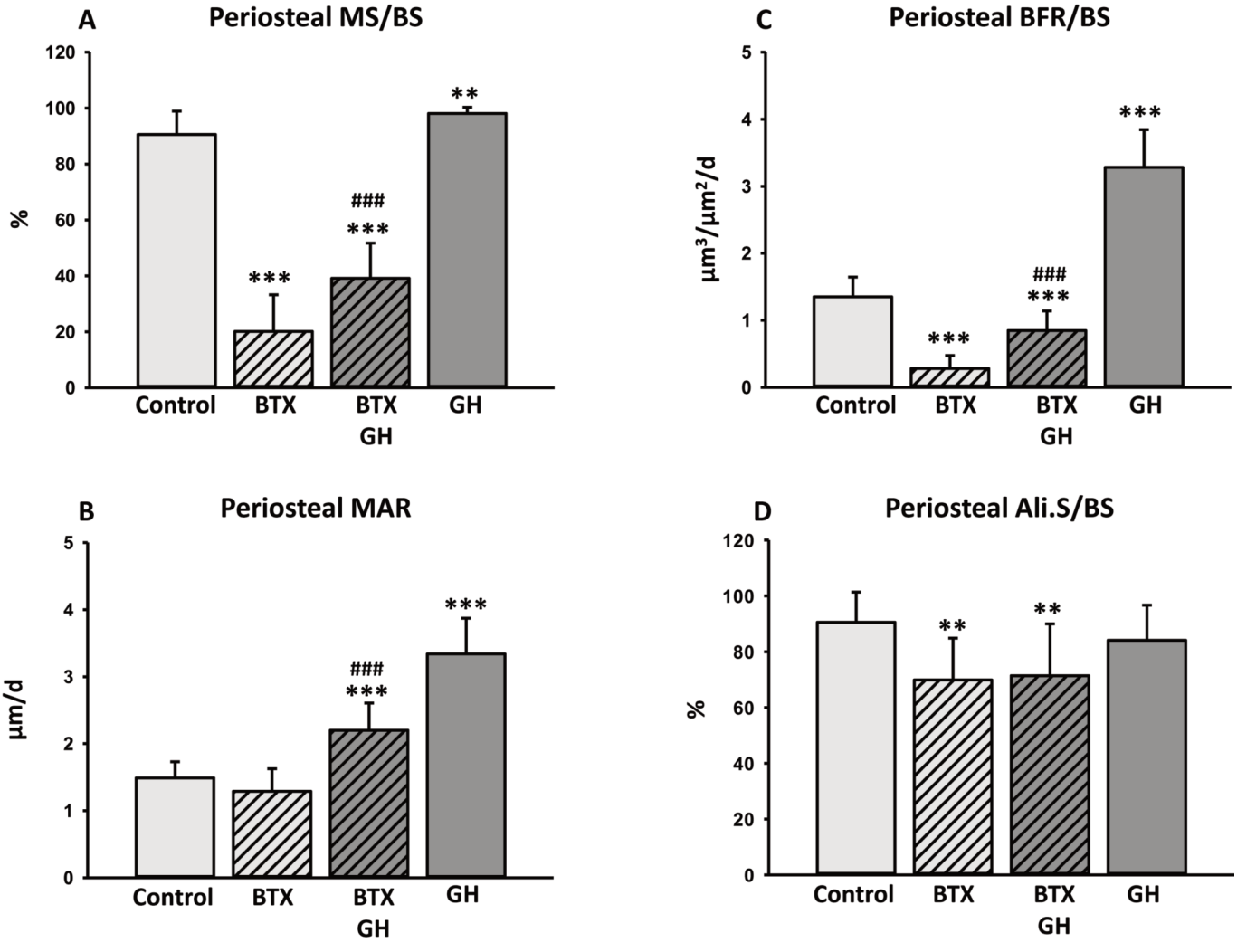

Figure 4. Dynamic histomorphometry on periosteal cortical bone (A) MS/BS, (B) MAR, (C) BFR/BS, and (D) Ali.S/BS from the mid-femur in rats with BTX induced hind limb paralysis treated with GH (5 mg/kg/d). Mean ± SD. **: $P<0.01$ vs. control ***: $P<0.001$ vs. control, ###: $P<0.001$ vs. BTX.

no differences in total area or marrow area were found between any of the groups, although the total area of BTX tended to be lower compared with the controls ($P=0.08$).

Dynamic histomorphometry of cortical bone

At the periosteal cortical bone surface BTX resulted in lower MS/BS (–78%, $P<0.001$), and BFR/BS (–79%, $P<0.001$) compared to controls (Figure 4A+C), whereas no difference in MAR was found (Figure 4B). In BTX+GH, MS/BS (–57%, $P<0.001$), and BFR/BS (–37%, $P<0.001$) were lower compared to controls, however, GH resulted in a 1-fold higher MS/BS ($P<0.001$) and a 2-fold higher BFR/BS ($P<0.001$) of the paralysed animals compared to BTX alone. In addition, GH resulted in 1-fold higher MAR ($P<0.001$) compared to controls and BTX. Furthermore, GH alone induced substantial higher MS/BS, MAR, and BFR/BS compared with controls (Figure 4D).

Ali.S/BS was lower in BTX (–23%, $P<0.01$) and BTX+GH (–21%, $P<0.01$) indicating an increased periosteal bone resorption in these groups during the experimental period.

No differences between the groups in MS/BS, MAR, BFR/BS, or Ali.S/BS at the endosteal surfaces were found (data not shown).

Discussion

The purpose of the present experiment was to study the efficacy of GH to counteract paralysis-induced loss of bone and muscle mass. The main findings were that treatment with GH mitigated paralysis-induced loss of periosteal bone formation and muscle mass. No effect of GH on trabecular BV/TV or bone strength was found.

BTX substantially reduced muscle mass and muscle cell CSA of the rectus femoris. This was accompanied by a substantial reduction of periosteal MS/BS as well as cross sectional bone area of the mid-femur, indicating that the fraction of periosteal surfaces with bone formation was decreased. However, no change of MAR was found, suggesting that at sites involving bone formation, the activity of the osteoblasts was not influenced by disuse. Furthermore, the lower amount of Ali.S/BS at the periosteal surfaces indicates that BTX increased bone resorption. Thus, disuse resulted in decreased bone formation as well in increased bone resorption at the periosteal surfaces leading to a reduced cross sectional bone area. Finally, in line with previous studies in rodents[11,12,28], disuse resulted in loss of femoral aBMD, trabecular BV/TV, trabecular thickness, and bone strength.

It is well known that GH induces growth[36]. In intact rodents, GH increases the circulating levels of IGF-I[37,38], as well as production of IGF-I locally in many tissues including bone[39]. GH and IGF-I are important during longitudinal bone growth, where these substances stimulates chondroblasts and chondrocytes located in the growth plate[40]. In the present study, disuse did not influence longitudinal bone growth as the femur length did not differ between control and paralysed animals. These findings support previous studies suggesting that short term unloading is not critical to longitudinally bone growth[12,41]. As expected, GH treatment of non-paralysed animals leads to increased femur length. Interestingly, the effect of GH on linear growth was not affected by disuse, as no differences in femur length between BTX+GH and GH alone were found. GH attenuated the loss of femoral BMC of the paralysed animals. In contrast, no differences in aBMD were found, indicating that the increase in BMC was due to an increased bone length due to GH administration.

GH treatment did not prevent loss of femoral trabecular BV/TV or thinning of the trabeculae. This is consistent with a previous study on hypophysectomised rats[25], where no effect on trabecular BV/TV was found neither when animals were treated with a replacement dose (GH: 500 μg/kg) or a pharmacological dose (GH: 5 mg/kg). Similar findings were reported in hindlimb suspended rats treated with IGF-I[42]. However, it should be noted that the duration of the above mentioned studies and of the present study is relatively short, and it is not known whether a longer treatment period with GH or IGF-I would influence BV/TV or trabecular thickness during disuse.

In long bones, GH is also known to influence bone width by stimulating periosteal bone formation[19,24]. In the present study, GH partially prevented BTX-induced loss of MS/BS and substantially increased MAR of the mid-femur, indicating that GH attenuated the loss of active osteoblasts and increased the bone forming activity of these osteoblasts to a level significantly above the controls. These findings are in accordance with studies of intact and unloaded hypophysectomised rats[19,24,25]. Nevertheless, the effect of GH on periosteal osteoblasts did not reduce BTX-induced loss of bone strength of the mid-femur. However, the experimental period was only 4 weeks, and it should be noted that GH alone did not influence the bone strength compared with controls. Thus, an extended experimental period is needed to ascertain whether GH can prevent loss of bone strength due to disuse.

The mechanisms behind disuse-induced bone loss are not fully elucidated, but the Wnt/β-catenin signalling pathway seems to be involved[43,44]. The Wnt/β-catenin signalling pathway is regulated by a number of molecules including sclerostin. Sclerostin is secreted by the osteocytes, and is suggested to inhibit bone formation by inhibiting osteoblastic Wnt/β-catenin signalling (for a review see[45]). The expression of the SOST gene encoding for sclerostin have been shown to be upregulated in tail suspended mice[43,44] and in mice with sciatic neurectomy-induced paralysis[46]. Furthermore, serum levels of sclerostin are increased in humans during bed rest[47]. Whether GH have any effect on the sclerostin production is not clear, however, serum levels of sclerostin seem to be decreased in acromegalic patients (personal communication, Dr. Tomris Erbas).

GH is a potent anabolic agent known to promote skeletal muscle cell protein synthesis and growth[22], which to a large extent is mediated by IGF-I[48]. In the present study, GH lead to a two-fold increase in serum IGF-I, and increased BW (21%) and muscle mass (m. rectus femoris and m. sternocleidomastoideus by 19%) of animals treated with GH alone, which is in agreement with previous studies[20,23,24,37]. The final BW of BTX-injected animals was decreased to a level significantly lower than that of control animals, which is in accordance with earlier studies[12,28]. GH treatment prevented the BTX-induced loss in body weight, which can be ascribed to the general anabolic effect of GH.

Muscle atrophy involves a reduction of the diameter of the muscle cells due to loss of mainly proteins (for review see[5]). IGF-I suppress protein degradation in muscle cells[5], and production of muscle IGF-I have been reported to be downregulated during unloading[49,50]. In the present study, GH could not prevent, but nevertheless attenuated the loss of rectus femoris muscle mass, which is in agreement with a previous study using a combination of GH and IGF-I in tail suspended rats[51]. This effect was accompanied by a diminished loss of muscle cell CSA, and may be mediated by the increased serum IGF-I as well as IGF-I produced locally in the muscle cells themselves. However, concentration of muscle IGF-I was not measured in the present study, but it has been demonstrated that GH administration increases skeletal muscle IGF-I mRNA production[52].

BTX severely affected the gait ability of the right hind limb of the animals and reached a minimum at day 5. However, this did not prevent the animals from moving freely around in the cages using the non-paralysed limbs, and they could easily access water and food during the entire experiment. GH did not influence the gait ability score at any time point.

The dosage of GH of 5 mg/kg/d used in the present study was selected, as previous studies using comparable GH dosages, have reported increased periosteal bone formation and bone strength[19,20]. The peak levels of endogenous GH in female rats reach 300-600 μg/l serum, and between peaks the levels are 20-100 μg/l[53]. When rats are injected subcutaneously with exogenous GH, a maximum peak level is reached after 2

hours. A dosage of 2 or 4 mg of GH per kg rat, results in peak levels of approximately 600 or 1200 μg/l serum, respectively[54]. The dosage of 5 mg/kg/day, divided into two daily doses, is a pharmacological dosage, resulting in relatively broad peaks twice a day.

In conclusion, the current study showed that GH mitigated disuse-induced loss of femoral periosteal bone formation and rectus femoris muscle mass. No effect of GH on femoral trabecular BV/TV or bone strength was found.

Acknowledgements

The authors are grateful for the excellent technical assistance of Jytte Utoft. GH was kindly donated by Novo Nordisk, and the μCT scanner was donated by the VELUX Foundation. The study was supported by The A.P. Møller Foundation for the Advancement of Medical Science, Aarhus University Research Foundation, and The Novo Nordisk Foundation. The Centre for Stochastic Geometry and Advanced Bioimaging is supported by the Villum Foundation. We thank Visiopharm for a contribution to the newCAST stereology software system.

References

1. Burge R, Dawson-Hughes B, Solomon DH, Wong JB, King A, Tosteson A. Incidence and economic burden of osteoporosis-related fractures in the United States, 2005-2025. J Bone Miner Res 2007;22:465-75.
2. Janssen I, Shepard DS, Katzmarzyk PT, Roubenoff R. The healthcare costs of sarcopenia in the United States. J Am Geriatr Soc 2004;52:80-5.
3. Marks R. Hip fracture epidemiological trends, outcomes, and risk factors, 1970-2009. Int J Gen Med 2010;3:1-17.
4. Harada S and Rodan GA. Control of osteoblast function and regulation of bone mass. Nature 2003;423:349-55.
5. Schiaffino S, Dyar KA, Ciciliot S, Blaauw B, Sandri M. Mechanisms regulating skeletal muscle growth and atrophy. FEBS J 2013;280:4294-314.
6. Vico L, Collet P, Guignandon A, Lafage-Proust MH, Thomas T, Rehaillia M, Alexandre C. Effects of long-term microgravity exposure on cancellous and cortical weight-bearing bones of cosmonauts. Lancet 2000; 355:1607-11.
7. Thomsen JS, Morukov BV, Vico L, Alexandre C, Saparin PI, Gowin W. Cancellous bone structure of iliac crest biopsies following 370 days of head-down bed rest. Aviat Space Environ Med 2005;76:915-22.
8. Wilmet E, Ismail AA, Heilporn A, Welraeds D, Bergmann P. Longitudinal study of the bone mineral content and of soft tissue composition after spinal cord section. Paraplegia 1995;33:674-7.
9. Shackelford LC, LeBlanc AD, Driscoll TB, Evans HJ, Rianon NJ, Smith SM, Spector E, Feeback DL, Lai D. Resistance exercise as a countermeasure to disuse-induced bone loss. J Appl Physiol 2004;97:119-29.
10. Chappard D, Chennebault A, Moreau M, Legrand E, Audran M, Basle MF. Texture analysis of X-ray radiographs is a more reliable descriptor of bone loss than mineral content in a rat model of localized disuse induced by the Clostridium botulinum toxin. Bone 2001;28:72-9.
11. Thomsen JS, Christensen LL, Vegger JB, Nyengaard JR, Brüel A. Loss of Bone Strength is Dependent on Skeletal Site in Disuse Osteoporosis in Rats. Calcif Tissue Int 2012;90:294-306.
12. Brüel A, Vegger JB, Raffalt AC, Andersen JET, Thomsen JS. PTH (1-34), but not strontium ranelate counteract loss of trabecular thickness and bone strength in disuse osteopenic rats. Bone 2013;53:51-8.
13. D'Ercole AJ, Stiles AD, Underwood LE. Tissue concentrations of somatomedin C: further evidence for multiple sites of synthesis and paracrine or autocrine mechanisms of action. Proc Natl Acad Sci U S A 1984;81:935-9.
14. Mason DJ, Hillam RA, Skerry TM. Constitutive *in vivo* mRNA expression by osteocytes of beta-actin, osteocalcin, connexin-43, IGF-I, c-fos and c-jun, but not TNF-alpha nor tartrate-resistant acid phosphatase. J Bone Miner Res 1996;11:350-7.
15. Slootweg MC, van Buul-Offers SC, Herrmann-Erlee MP, van der Meer JM, Duursma SA. Growth hormone is mitogenic for fetal mouse osteoblasts but not for undifferentiated bone cells. J Endocrinol 1988;116:R11-R13.
16. Kassem M, Blum W, Ristelli J, Mosekilde L, Eriksen EF. Growth hormone stimulates proliferation and differentiation of normal human osteoblast-like cells *in vitro*. Calcif Tissue Int 1993;52:222-6.
17. Zhang W, Shen X, Wan C, Zhao Q, Zhang L, Zhou Q, Deng L. Effects of insulin and insulin-like growth factor 1 on osteoblast proliferation and differentiation: differential signalling via Akt and ERK. Cell Biochem Funct 2012; 30:297-302.
18. Spencer EM, Liu CC, Si EC, Howard GA. *In vivo* actions of insulin-like growth factor-I (IGF-I) on bone formation and resorption in rats. Bone 1991;12:21-6.
19. Ortoft G, Andreassen TT, Oxlund H. Growth hormone increases cortical and cancellous bone mass in young growing rats with glucocorticoid-induced osteopenia. J Bone Miner Res 1999;14:710-21.
20. Ortoft G, Brüel A, Andreassen TT, Oxlund H. Growth hormone is not able to counteract osteopenia of rat cortical bone induced by glucocorticoid with protracted effect. Bone 1995;17:543-8.
21. Andreassen TT and Oxlund H. The influence of combined parathyroid hormone and growth hormone treatment on cortical bone in aged ovariectomized rats. J Bone Miner Res 2000;15:2266-75.
22. Ullman M and Oldfors A. Effects of growth hormone on skeletal muscle. I. Studies on normal adult rats. Acta Physiol Scand 1989;135:531-6.
23. Ortoft G, Gronbaek H, Oxlund H. Growth hormone administration can improve growth in glucocorticoid-injected rats without affecting the lymphocytopenic effect of the glucocorticoid. Growth Horm IGF Res 1998;8:251-64.
24. Andreassen TT, Jorgensen PH, Flyvbjerg A, Orskov H,

Oxlund H. Growth hormone stimulates bone formation and strength of cortical bone in aged rats. J Bone Miner Res 1995;10:1057-67.
25. Halloran BP, Bikle DD, Harris J, Autry CP, Currier PA, Tanner S, Patterson-Buckendahl P, Morey-Holton E. Skeletal unloading induces selective resistance to the anabolic actions of growth hormone on bone. J Bone Miner Res 1995;10:1168-76.
26. Bikle DD, Harris J, Halloran BP, Currier PA, Tanner S, Morey-Holton E. The molecular response of bone to growth hormone during skeletal unloading: regional differences. Endocrinology 1995;136:2099-109.
27. Sakata T, Wang Y, Halloran BP, Elalieh HZ, Cao J, Bikle DD. Skeletal unloading induces resistance to insulin-like growth factor-I (IGF-I) by inhibiting activation of the IGF-I signaling pathways. J Bone Miner Res 2004; 19:436-46.
28. Warner SE, Sanford DA, Becker BA, Bain SD, Srinivasan S, Gross TS. Botox induced muscle paralysis rapidly degrades bone. Bone 2006;38:257-64.
29. Gundersen HJG and Jensen EB. The efficiency of systematic sampling in stereology and its prediction. J Microsc 1987;147:229-63.
30. Gundersen HJG. The nucleator. J Microsc 1988;151:3-21.
31. Bouxsein ML, Boyd SK, Christiansen BA, Guldberg RE, Jepsen KJ, Muller R. Guidelines for assessment of bone microstructure in rodents using micro-computed tomography. J Bone Miner Res 2010;25:1468-86.
32. Thomsen JS, Laib A, Koller B, Prohaska S, Mosekilde L, Gowin W. Stereological measures of trabecular bone structure: comparison of 3D micro computed tomography with 2D histological sections in human proximal tibial bone biopsies. J Microsc 2005;218:171-9.
33. Oxlund H and Andreassen TT. Simvastatin treatment partially prevents ovariectomy-induced bone loss while increasing cortical bone formation. Bone 2004;34:609-18.
34. Dempster DW, Compston JE, Drezner MK, Glorieux FH, Kanis JA, Malluche H, Meunier PJ, Ott SM, Recker RR, Parfitt AM. Standardized nomenclature, symbols, and units for bone histomorphometry: a 2012 update of the report of the ASBMR Histomorphometry Nomenclature Committee. J Bone Miner Res 2013;28:2-17.
35. Vegger JB, Nielsen ES, Bruel A, Thomsen JS. Additive effect of PTH (1-34) and zoledronate in the prevention of disuse osteopenia in rats. Bone 2014;66:287-95.
36. Andreassen TT and Oxlund H. The effects of growth hormone on cortical and cancellous bone. J Musculoskelet Neuronal Interact 2001;2:49-58.
37. Brüel A, Oxlund H, Nyengaard JR. The total length of myocytes and capillaries, and total number of myocyte nuclei in the rat heart are time-dependently increased by growth hormone. Growth Horm IGF Res 2005;15:256-64.
38. Brüel A, Oxlund H, Nyengaard JR. Growth hormone increases the total number of myocyte nuclei in the left ventricle of adult rats. Growth Horm IGF Res 2002; 12:106-15.
39. Isgaard J, Moller C, Isaksson OG, Nilsson A, Mathews LS, Norstedt G. Regulation of insulin-like growth factor messenger ribonucleic acid in rat growth plate by growth hormone. Endocrinology 1988;122:1515-20.
40. Hunziker EB, Wagner J, Zapf J. Differential effects of insulin-like growth factor I and growth hormone on developmental stages of rat growth plate chondrocytes *in vivo*. J Clin Invest 1994;93:1078-86.
41. Sibonga JD, Zhang M, Evans GL, Westerlind KC, Cavolina JM, Morey-Holton E, Turner RT. Effects of spaceflight and simulated weightlessness on longitudinal bone growth. Bone 2000;27:535-40.
42. Boudignon BM, Bikle DD, Kurimoto P, Elalieh H, Nishida S, Wang Y, Burghardt A, Majumdar S, Orwoll BE, Rosen C, Halloran BP. Insulin-like growth factor I stimulates recovery of bone lost after a period of skeletal unloading. J Appl Physiol (1985) 2007;103:125-31.
43. Lin C, Jiang X, Dai Z, Guo X, Weng T, Wang J, Li Y, Feng G, Gao X, He L. Sclerostin mediates bone response to mechanical unloading through antagonizing Wnt/beta-catenin signaling. J Bone Miner Res 2009;24:1651-61.
44. Robling AG, Niziolek PJ, Baldridge LA, Condon KW, Allen MR, Alam I, Mantila SM, Gluhak-Heinrich J, Bellido TM, Harris SE, Turner CH. Mechanical stimulation of bone *in vivo* reduces osteocyte expression of Sost/sclerostin. J Biol Chem 2008;283:5866-75.
45. Baron R and Kneissel M. WNT signaling in bone homeostasis and disease: from human mutations to treatments. Nat Med 2013;19:179-92.
46. Moustafa A, Sugiyama T, Prasad J, Zaman G, Gross TS, Lanyon LE, Price JS. Mechanical loading-related changes in osteocyte sclerostin expression in mice are more closely associated with the subsequent osteogenic response than the peak strains engendered. Osteoporos Int 2012;23:1225-34.
47. Frings-Meuthen P, Boehme G, Liphardt AM, Baecker N, Heer M, Rittweger J. Sclerostin and DKK1 levels during 14 and 21 days of bed rest in healthy young men. J Musculoskelet Neuronal Interact 2013;13:45-52.
48. Vijayakumar A, Buffin NJ, Gallagher EJ, Blank J, Wu Y, Yakar S, LeRoith D. Deletion of growth hormone receptors in postnatal skeletal muscle of male mice does not alter muscle mass and response to pathological injury. Endocrinology 2013;154:3776-83.
49. Hanson AM, Harrison BC, Young MH, Stodieck LS, Ferguson VL. Longitudinal characterization of functional, morphologic, and biochemical adaptations in mouse skeletal muscle with hindlimb suspension. Muscle Nerve 2013;48:393-402.
50. Han B, Zhu MJ, Ma C, Du M. Rat hindlimb unloading down-regulates insulin like growth factor-1 signaling and AMP-activated protein kinase, and leads to severe atrophy of the soleus muscle. Appl Physiol Nutr Metab 2007;32:1115-23.
51. Allen DL, Linderman JK, Roy RR, Grindeland RE, Mukku V, Edgerton VR. Growth hormone/IGF-I and/or

resistive exercise maintains myonuclear number in hindlimb unweighted muscles. J Appl Physiol 1997; 83:1857-61.
52. Gosteli-Peter MA, Winterhalter KH, Schmid C, Froesch ER, Zapf J. Expression and regulation of insulin-like growth factor-I (IGF-I) and IGF-binding protein messenger ribonucleic acid levels in tissues of hypophysectomized rats infused with IGF-I and growth hormone. Endocrinology 1994;135:2558-67.
53. Clark RG, Carlsson LM, Robinson IC. Growth hormone secretory profiles in conscious female rats. J Endocrinol 1987;114:399-407.
54. Jorgensen PH, Bang C, Andreassen TT, Flyvbjerg A, Orskov H. Dose-response study of the effect of growth hormone on mechanical properties of skin graft wounds. J Surg Res 1995;58:295-301.